Evaluation of D-Isomers of O-^{11}C-Methyl Tyrosine and O-^{18}F-Fluoromethyl Tyrosine as Tumor-Imaging Agents in Tumor-Bearing Mice: Comparison with L- and D-^{11}C-Methionine

Hideo Tsukada, PhD; Kengo Sato, MS; Dai Fukumoto, BA; Shingo Nishiyama, MS; Norihiro Harada, MS; and Takeharu Kakiuchi, PhD

PET Center, Central Research Laboratory, Hamamatsu Photonics K.K., Hamamatsu, Shizuoka, Japan

The aim of this study was to investigate whether D-amino acid isomers of O-^{11}C-methyl tyrosine (^{11}C-CMT) and O-^{18}F-fluoromethyl tyrosine (^{18}F-FMT) were better than the corresponding L-isomers as tumor- detecting agents with PET in comparison with the difference between L- and D-methyl-^{11}C-methionine (^{11}C-MET). **Methods:** L- and D-^{11}C-MET, ^{11}C-CMT, and ^{18}F-FMT were injected intravenously into BALB/cA Jcl-nu mice bearing HeLa tumor cells. At 5, 15, 30, and 60 min after injection, normal abdominal organs and xenotransplanted HeLa cells were sampled, and the uptake of each ligand was determined. Metabolic analyses of these compounds in the plasma were also performed. Accumulation of the D-isomers of ^{11}C-MET, ^{11}C-CMT, and ^{18}F-FMT in turpentine-induced inflammatory tissue was assayed in comparison with ^{18}F-FDG. The whole-body distribution of each tracer was imaged with a planar positron imaging system (PPIS). **Results:** Although the tumor uptake (standardized uptake value [SUV]) levels of the D-isomers of ^{11}C-MET, ^{11}C-CMT, and ^{18}F-FMT were 261%, 72%, and 95% of each L-isomer 60 min after administration, the tumor-to-blood ratios of these D-isomers were 130%, 140%, and 182% of the corresponding L-isomers. In the blood, the D-isomers of these labeled compounds revealed a relatively faster elimination rate compared with their L-isomers, with a high peak uptake in the blood and kidney 5 min after administration. Compared with the natural amino acid ligand L-^{11}C-MET, the uptake of L-isomers of ^{11}C-CMT and ^{18}F-FMT was relatively low and stable in the abdominal organs, whereas D-isomers revealed much lower levels and faster clearance rates compared with corresponding L-isomers. Among the abdominal organs, the pancreas showed a relatively high uptake of ^{11}C-CMT and ^{18}F-FMT; the uptake of these D-isomers was much lower than that of L-isomers. Pretreatment with cycloheximide, a protein synthesis inhibitor, resulted in a marked reduction of L-^{11}C-MET uptake and a slight reduction of D-^{11}C-MET uptake into protein fractions, whereas no significant changes were detected with L- and D-^{11}C-CMT and ^{18}F-FMT. D-Isomers of ^{11}C-MET, ^{11}C-CMT, and ^{18}F-FMT did not accumulate in turpentine-induced inflammatory tissue, where ^{18}F-FDG revealed a high uptake. Whole-body imaging with a PPIS provided consistent distribution data obtained from the tissue dissection analysis. **Conclusion:** These results suggest that D-isomers of ^{11}C-CMT and ^{18}F-FMT could be potentially better tracers than L- and D-^{11}C-MET for tumor imaging with PET.

Key Words: D-amino acids; ^{11}C-methionine; O-^{11}C-methyl tyrosine; O-^{18}F-fluoromethyl tyrosine; tumor imaging

J Nucl Med 2006; 47:679–688

Although PET imaging with ^{18}F-FDG is routinely used for tumor detection and therapy monitoring, several limitations have been reported with ^{18}F-FDG, such as a high uptake in the normal tissue of the brain and in inflammatory tissues (*1*). In contrast, because of the low rate of amino acid use in the cortical normal tissues, positron-labeled amino acids and their analogs are considered to be useful, especially for tumor detection in the brain. Their use in tumor detection is based primarily on an increased cellular uptake of amino acids, which is assumed to reflect an enhanced amino acid transporter, metabolism, and protein synthesis. Natural and unnatural artificial labeled amino acids—1-^{11}C-methionine (*2,3*), methyl-^{11}C-methionine (^{11}C-MET) (*3–5*), 1-^{11}C-tyrosine (*6,7*), β-^{11}C-tyrosine (^{11}C-TYR) (*8*), 1-^{11}C-leucine (^{11}C-LEU) (*9*), 1-^{11}C-phenylalanine (^{11}C-PHE) (*10,11*), 4-^{18}F-fluoro-L-phenylalanine (*12*), and 2-^{18}F-fluoro-L-tyrosine (*13,14*)—have been proposed (*15*). Among these labeled amino acids, L-^{11}C-MET is widely used for tumor imaging with PET. Because it has been reported that L-^{11}C-MET is incorporated not only into protein fractions via the conversion into amino-acyl-tRNA (tRNA is transfer RNA) but also into nonprotein materials, such as lipids and RNA, by the transmethylation process via *S*-adenosyl-L-methionine (*3*), the value of this tracer is considered as a marker of methionine transport into the tissue in vivo for imaging tumor tissues with PET (*15*). Influenced by this working hypothesis, several artificial and unnatural amino acid tracers—O-^{11}C-methyl-L-tyrosine (CMT) (*16,17*), O-^{18}F-fluoromethyl-L-tyrosine (FMT) (*16,17*), O-^{18}F-fluoroethyl-L-tyrosine

(FET) (18,19), O-^{18}F-fluoropropyl-L-tyrosine (20,21), ^{11}C-ethionine (22), and ^{11}C-propionine (22)—were synthesized and their potential to be better tumor-imaging agents was evaluated. These radiolabeled compounds were found to behave as unnatural amino acids after intravenous injection, exhibiting almost no incorporation into the protein fraction and relatively low accumulation, with no significant elevation of the radioactivity with time in normal peripheral tissues (low tissue-to-blood ratio). These compounds also showed relatively slow blood clearance and relatively high uptake into tumor tissue (high tumor-to-blood ratio).

Because L-isomers of amino acids are commonly used in mammalian cells in nature, D-isomers are considered to be unnatural amino acids, and radiolabeled D-amino acids are expected to be good tumor-imaging agents. However, the results have been somewhat controversial. It has been reported that D-isomers of some radiolabeled amino acids, such as ^{14}C-MET (23) and ^{14}C-LEU (24), showed higher uptake into the pancreas and xenotransplanted tumor cells than that of the corresponding L-isomers. On the other hand, D-^{18}F-FET revealed negligible accumulation in human colon carcinoma cells in the in vitro assay (19), as well as in mouse brain (18), compared with its L-isomer. Schober et al. (25) showed no selective transport of L- and D-^{11}C-MET into a malignant glioma; however, Bergström et al. (26) demonstrated that the uptake of D-^{11}C-MET into brain tumors was lower than that of L-^{11}C-MET.

The aim of this study was to evaluate the potential of the D-isomers of ^{11}C-CMT and ^{18}F-FMT as tumor-imaging agents in comparison with their corresponding L-isomers as well as L- and D-^{11}C-MET in tumor-bearing mice. In addition to the tissue dissection method, the biodistribution and kinetics of each radiolabeled compound in mice were determined by a planar positron imaging system (PPIS) (27).

MATERIALS AND METHODS

Animals

Female BALB/cA Jcl-nu mice (6-wk old) were obtained from Japan Clea. Mice were housed, 5 animals per cage, under standard laboratory conditions at 25°C and 50% humidity with a 12-h light/dark cycle (light on at 6:00 AM, light off at 6:00 PM) throughout the experimental period. They were allowed free access to food and water. Mice at 7 wk of age were inoculated subcutaneously with 5×10^6 JCRB9004 HeLa cells (doubling time, 4.4 d), maintained for 2 wk after xenotransplantation while monitoring the growth rate, and subjected to experiments at 9 wk of age. Mice were maintained and handled in accordance with the recommendations of the National Institutes of Health and also the guidelines of the Central Research Laboratory, Hamamatsu Photonics K.K.

Chemicals

FDG, L- and D-homocysteine thiolactone, L- and D-MET, and D-tyrosine were purchased from Sigma-Aldrich. Cycloheximide, trichloroacetic acid (TCA), and turpentine oil were from Wako Pure Chemical Industry. 4,7,13,16,21,24-Hexaoxa-1,10-diazabicyclo-[8,8,8]hexacosane (Kryptofix 2.2.2.) and $K_2CO_3 \cdot 1.5$ H_2O were from Merck. L-Tyrosine and methyl iodide were obtained from

Nacalai Tesque, and mannose triflate was obtained from ABX. All other reagents were of analytic grade.

L- and D-isomers of CMT and FMT were synthesized by reactions of methyl iodide and fluoromethyl bromide with the corresponding L- and D-tyrosine.

Syntheses of Labeled Compounds

Positron-emitting ^{11}C and ^{18}F were produced by ^{14}N(p,α)^{11}C and ^{18}O(p,n)^{18}F nuclear reactions, respectively, using the cyclotron (HM-18; Sumitomo Heavy Industry) at Hamamatsu Photonics PET Center.

^{11}C-Methyl iodide was prepared from ^{11}C-CO_2. L- and D-^{11}C-MET was labeled by S-methylation of L- and D-homocysteine thiolactone, respectively (4).

L- or D-^{11}C-CMT was prepared by reactions of ^{11}C-methyl iodide with the corresponding L- and D-tyrosine. (16).

L- or D-^{18}F-FMT was synthesized by reactions of ^{18}F-fluoromethyl bromide with the corresponding L- and D-tyrosine according to a previous report, with minor modifications (16). After irradiation, ^{18}F-fluoride was recovered from the target by He flow. The recovered ^{18}F-fluoride solution was then trapped on an ion-exchange resin (AG1-X8; Bio-Rad) and eluted from the resin by 0.5 mL of 40 mmol/L K_2CO_3 solution. To this fluoride solution, 2 mL of Kryptofix 2.2.2. solution (containing 15 mg of Kryptofix 2.2.2. in CH_3CN) was added. Water was removed by azeotropic distillation at 110°C under He flow (400 mL/min) for 5 min. To the residue, the addition of acetonitrile (1 mL) and azeotropic distillation were repeated twice. Then, the residue was dried under reduced pressure for 1 min and under He flow (50 mL/min) for 1 min. Cooling the residue to room temperature gave the activated ^{18}F-fluoride/Kryptofix 2.2.2. complex. To synthesize the no-carrier-added 2-^{18}F-fluoromethyl bromide (^{18}F-FMBr), 0.1 mL of dibromomethane in 1 mL of CH_3CN was added to the ^{18}F-fluoride/Kryptofix 2.2.2. complex and reacted at 110°C for 4 min. ^{18}F-FMBr was distilled into the precursor solution through in-line connected Sep-Pak silica cartridges (Waters). Then, ^{18}F-fluoromethylation with ^{18}F-FMBr was performed using the same procedure as that for ^{11}C-alkylation as described.

Enantiomeric purity was analyzed on a CHIOBIOTIC T column (4.6 mm × 250 mm; Tokyo Kasei Kogyo). The elution solution was ethanol/water (1:1), and the flow rate was 1 mL/min.

The production of ^{18}F-FDG was performed according to a method described elsewhere (28).

Tissue Distribution Assay

Five megabecquerels of a radiolabeled compound were injected into each mouse the through tail vein. The animals were killed by decapitation under halothane anesthesia at 5, 15, 30, and 60 min after the injection; samples of blood, heart, lung, liver, pancreas, kidney, spleen, small intestine, gut, and tumor were rapidly removed, and the weight and radioactivity were measured using a γ-counter (ARC-2000; Aloka). Standardized uptake values (SUVs) were calculated as the radioactivity in tissue divided by the ratio of the total injected radioactivity and the body weight. For metabolite analysis, blood samples were centrifuged to separate the plasma and weighed, and the radioactivity was measured; methanol was then added to some plasma samples (sample/methanol, 1:1) and centrifuged, and the supernatants were developed on thin-layer chromatography (TLC) plates (AL SIL G/UV; Whatman) using a mobile phase of n-buthanol/acetic acid/phosphate-buffered saline ([PBS] pH 7.4; 4:1:2). At each sampling time point for analysis, the ratio of radioactivity in the unmetabolized fraction to that in the total plasma

(metabolized plus unmetabolized) was determined using a phosphoimaging plate (BAS-1500 MAC; Fuji Photo Films Co., Ltd.).

Incorporation of Radiolabeled Ligands into Proteins

For inhibition of protein synthesis, saline or cycloheximide (100 mg/kg body weight) was administered intraperitoneally 30 min before tracer injection; animals were killed 60 min after injection. Incorporation of L- and D-^{11}C-MET, ^{11}C-CMT, and ^{18}F-FMT into the proteins was measured in the tumor, liver, pancreas, and plasma. Tissues obtained 60 min after tracer administration were immediately homogenized in 7.5% TCA with an ice-cold Teflon–glass homogenizer (Teflon; DuPont) and centrifuged at 7,500g for 5 min. The precipitate was washed 2 more times, and all supernatant fractions were collected as an acid-soluble fraction (ASF). The radioactivity in the ASF and in the final acid-precipitable fraction (APF) was counted using a γ-counter to determine the protein incorporation ratio (PIR [%] = $RI_{APF}/[RI_{ASF} + RI_{APF}] \times 100$ [where RI is radioisotope]).

Whole-Body Imaging of Tumor-Bearing Mice

Kinetics and distribution patterns of each radiolabeled compound were determined with a PPIS (Hamamatsu Photonics K.K.) (27). A planar imaging system for positron-emitting radiotracers consists of 2 opposing planar detectors, each having 4 (columns) × 6 (rows) detector units, and each unit composed of 10×10 arrays of $2 \times 2 \times 20$ mm^3 pillars of $Bi_4Ge_3O_{12}$ (BGO) scintillators and a metal-packaged position-sensitive photomultiplier tube. Focal plane images are constructed from coincidence data collected by opposing planar detectors, achieving data acquisition with higher sensitivity and finer spatial resolution than conventional PET (27). Two mice anesthetized with chloral hydrate were positioned prone on an acrylic plate and placed on the midplane between the 2 opposing detectors arranged in a horizontal mode. Each radiolabeled compound at a dose of 1 MBq was injected intravenously into each mouse from the tail vein. The data were acquired with a 1-min time frame interval for 60 min, and 6 summation images were created every 10 min.

Inflammation Model

For evaluation of tracer accumulations in the inflammatory tissue, mice were administered subcutaneously with 0.05 mL of turpentine oil, and the tracer uptake was measured 3 d after turpentine oil injection (29). The mice were imaged with a PPIS for 60 min after the injection of ^{18}F-FDG and D-isomers of ^{11}C-MET, ^{11}C-CMT, and ^{18}F-FMT.

Statistical Analysis

Results are expressed as mean ± SD. Comparisons between conditions were performed using the unpaired, 2-tailed Student t test. $P < 0.05$ was considered to indicate statistical significance.

RESULTS

To evaluate the D-isomers of amino acid analogs as tumor-detecting agents, the quality control of enantiomeric purity was a very critical factor. The retention times determined on enantiomeric analytic high-performance liquid chromatography (HPLC) were L- and D-MET, 4.71 and 6.28 min; L- and D-CMT, 5.65 and 7.12 min; and L- and D-FMT, 5.16 and 6.74 min, respectively. As shown in Figure 1, the enantiomeric purities of these 6 radiolabeled compounds were >98%.

The tissue distribution and kinetics of the L- and D-isomers of ^{11}C-MET, ^{11}C-CMT, and ^{18}F-FMT in HeLa-bearing mice are summarized in Tables 1–3. The SUVs of D-^{11}C-MET in the blood were higher than those of L-^{11}C-MET throughout the study, decreasing gradually with time after the injection (Table 1). In contrast, although the D-isomers of ^{11}C-CMT and ^{18}F-FMT revealed higher peak levels in the blood 5 min after injection, followed by faster elimination rates than the corresponding L-isomers, the resulting blood levels of the D-isomers were lower than those of the corresponding L-isomers 15 min and later after injection (Tables 2 and 3). When compared at 60 min after injection, the tumor uptake values (SUVs) and tumor-to-blood ratios of these 3 D-isomers were greater than those of ^{18}F-FDG (Table 4).

Metabolic analysis of the plasma demonstrated that L-^{11}C-MET was rapidly metabolized, whereas D-^{11}C-MET remained in the unmetabolized form up to 60 min after injection (Fig. 2A). Although both isomers of ^{11}C-CMT and ^{18}F-FMT were remarkably stable, the D-isomers indicated slightly more stable profiles in the plasma than those of the L-isomers (Figs. 2B and 2C).

The uptake of D-^{11}C-MET was lower in the liver, gut, and intestine and higher in the kidney and muscle compared with that of L-^{11}C-MET throughout the study (Table 1). Of interest, the uptake of D-^{11}C-MET in the brain was significantly higher than that of L-^{11}C-MET 60 min after injection (Table 1). Compared with the natural amino acid
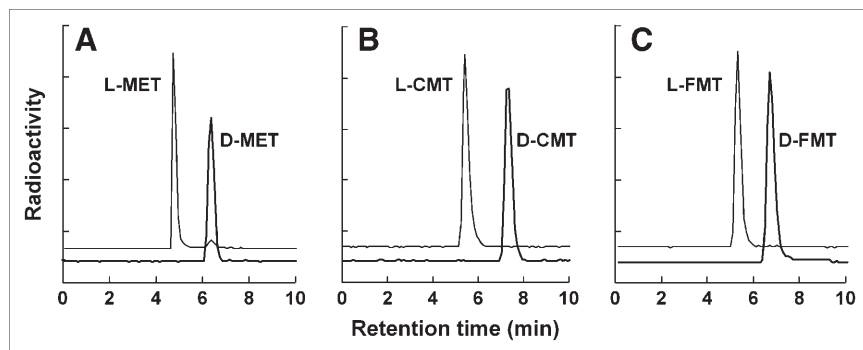
FIGURE 1. HPLC analyses of enantiomeric purities of L- and D-isomers of ^{11}C-MET (A), ^{11}C-CMT (B), and ^{18}F-FMT (C). Enantiomeric purity of each compound was analyzed on a CHIOBIOTIC T column using an elution solution of ethanol/water (1:1) at a flow rate of 1 mL/min.

TABLE 1
Uptake of L- and D-^{11}C-MET in Tumor-Bearing Mice

Organ	Isomer	5 min	15 min	30 min	60 min
Blood	L	0.593 ± 0.027	0.300 ± 0.017	0.256 ± 0.016	0.260 ± 0.017
	D	1.365 ± 0.029	0.855 ± 0.053	0.610 ± 0.010	0.523 ± 0.064
Heart	L	1.329 ± 0.062	0.940 ± 0.155	0.756 ± 0.005	0.710 ± 0.020
	D	1.315 ± 0.103	1.208 ± 0.040	1.033 ± 0.031	0.798 ± 0.033
Lung	L	1.196 ± 0.068	0.994 ± 0.141	0.998 ± 0.025	0.900 ± 0.035
	D	1.409 ± 0.070	1.100 ± 0.007	1.020 ± 0.023	0.950 ± 0.014
Liver	L	3.117 ± 0.186	4.350 ± 0.788	4.222 ± 0.311	4.755 ± 0.792
	D	1.469 ± 0.138	1.844 ± 0.129	2.282 ± 0.081	3.184 ± 0.066
Kidney	L	1.973 ± 0.023	2.120 ± 0.192	1.992 ± 0.180	1.961 ± 0.051
	D	2.458 ± 0.046	2.872 ± 0.408	2.906 ± 0.270	3.573 ± 0.110
Spleen	L	1.666 ± 0.125	1.489 ± 0.164	1.904 ± 0.212	1.631 ± 0.166
	D	1.740 ± 0.132	1.522 ± 0.115	1.575 ± 0.061	1.660 ± 0.184
Muscle	L	0.744 ± 0.020	0.621 ± 0.047	0.524 ± 0.022	0.381 ± 0.021
	D	0.619 ± 0.013	0.696 ± 0.045	0.699 ± 0.027	0.607 ± 0.037
Bone	L	0.914 ± 0.031	0.980 ± 0.130	0.924 ± 0.068	0.919 ± 0.045
	D	0.893 ± 0.104	0.836 ± 0.034	0.867 ± 0.038	0.822 ± 0.047
Intestine	L	1.978 ± 0.295	1.988 ± 0.623	2.945 ± 0.373	2.807 ± 0.067
	D	1.230 ± 0.125	1.187 ± 0.052	1.417 ± 0.126	1.765 ± 0.085
Gut	L	1.013 ± 0.084	1.077 ± 0.151	1.291 ± 0.045	1.281 ± 0.086
	D	0.802 ± 0.107	0.767 ± 0.082	0.829 ± 0.074	0.872 ± 0.033
Pancreas	L	5.635 ± 1.171	7.098 ± 1.058	7.819 ± 0.905	7.626 ± 0.982
	D	8.279 ± 2.260	7.931 ± 1.870	6.441 ± 0.042	7.358 ± 0.493
Brain	L	ND	ND	ND	0.495 ± 0.028
	D	ND	ND	ND	0.795 ± 0.114
Tumor	L	1.560 ± 0.326	1.348 ± 0.204	1.292 ± 0.254	1.182 ± 0.324
	D	1.952 ± 0.253	2.829 ± 0.074	2.887 ± 0.241	3.087 ± 0.487

ND = not determined.

Mice ($n = 5$ at each time point) were injected intravenously with 5 MBq of L- or D-^{11}C-MET via tail vein and killed at 5, 15, 30, and 60 min after injection; tissue samples were rapidly removed, and weight and radioactivity were measured. Data are expressed as SUV.

ligand L-^{11}C-MET, the uptake of the L-isomers of ^{11}C-CMT and ^{18}F-FMT was relatively low and stable in the abdominal organs, and also the D-isomers revealed much lower and faster clearance rates compared with the corresponding L-isomers, except in the kidney and liver at the early phase (Tables 2 and 3). In parallel with the blood kinetics, the uptake of the D-isomers of ^{11}C-CMT and ^{18}F-FMT in the kidney was initially much higher up to 15 min after injection and lower 30 min and later after injection than that of the corresponding L-isomers (Tables 2 and 3). Compared with the L-isomers of these labeled compounds, the kinetics of these 2 D-isomers in the liver were also higher 5 min after injection and lower thereafter (Tables 2 and 3). Among the abdominal organs, the pancreas showed a remarkably high uptake of all labeled compounds used here; however, the uptake of the D-isomers of ^{11}C-CMT and ^{18}F-FMT was much lower than that of the L-isomers (Tables 2 and 3). In contrast to the enantiomeric difference of ^{11}C-MET, the brain uptake of the D-isomers of ^{11}C-CMT and ^{18}F-FMT was lower than that of the corresponding L-isomers (Tables 2 and 3).

As for the enantiomeric difference of each amino acid analog in the tumor tissue, D-^{11}C-MET showed a higher uptake (SUV) in tumor tissues than that of its L-isomer throughout the period up to 60 min after injection, showing 261% of its L-isomer 60 min after injection (Table 1). When the tumor uptake was expressed as the tumor-to-blood ratio, D-^{11}C-MET showed a gradual increase with time up to 60 min after injection, with lower values than its L-isomer until 30 min after injection, followed by a higher value thereafter because of the declining curve of L-^{11}C-MET, resulting in the ratio of the D-isomer being 130% of the L-isomer 60 min after injection (Fig. 3A). In contrast, the tumor uptake (SUV) levels of the D-isomers of ^{11}C-CMT and ^{18}F-FMT were relatively lower (about 72% and 95%, respectively, at 60 min after injection) than those of the corresponding L-isomers throughout the analysis (Tables 2 and 3); however, the tumor-to-blood ratios of these D-isomers were 140% and 182% of the corresponding L-isomers (Figs. 3B and 3C). To observe the contrast to the abdominal organ, the tumor-to-liver ratios were compared among these labeled compounds.

TABLE 2
Uptake of L- and D-^{11}C-CMT in Tumor-Bearing Mice

Organ	Isomer	5 min	15 min	30 min	60 min
Blood	L	1.229 ± 0.018	1.035 ± 0.018	0.927 ± 0.053	0.783 ± 0.041
	D	1.650 ± 0.027	0.769 ± 0.030	0.482 ± 0.024	0.405 ± 0.032
Heart	L	1.334 ± 0.024	1.053 ± 0.049	0.900 ± 0.015	0.839 ± 0.028
	D	1.193 ± 0.102	0.941 ± 0.006	0.627 ± 0.056	0.406 ± 0.023
Lung	L	1.241 ± 0.051	1.069 ± 0.088	0.882 ± 0.008	0.812 ± 0.021
	D	1.654 ± 0.032	1.044 ± 0.050	0.612 ± 0.077	0.382 ± 0.054
Liver	L	0.997 ± 0.007	0.846 ± 0.027	0.761 ± 0.012	0.650 ± 0.030
	D	1.626 ± 0.017	0.750 ± 0.030	0.441 ± 0.032	0.361 ± 0.029
Kidney	L	1.277 ± 0.049	1.177 ± 0.099	1.058 ± 0.074	0.918 ± 0.117
	D	3.972 ± 0.359	1.522 ± 0.114	0.946 ± 0.115	0.685 ± 0.140
Spleen	L	1.556 ± 0.075	1.349 ± 0.066	1.422 ± 0.064	1.174 ± 0.122
	D	1.188 ± 0.225	1.012 ± 0.117	0.795 ± 0.179	0.700 ± 0.138
Muscle	L	1.156 ± 0.016	0.960 ± 0.052	0.846 ± 0.049	0.711 ± 0.031
	D	0.551 ± 0.026	0.526 ± 0.007	0.517 ± 0.036	0.462 ± 0.033
Bone	L	0.887 ± 0.032	0.753 ± 0.085	0.659 ± 0.011	0.630 ± 0.017
	D	0.684 ± 0.043	0.532 ± 0.013	0.395 ± 0.041	0.313 ± 0.025
Intestine	L	1.156 ± 0.066	0.982 ± 0.048	0.926 ± 0.070	0.869 ± 0.038
	D	1.084 ± 0.047	0.739 ± 0.011	0.484 ± 0.081	0.314 ± 0.010
Gut	L	0.751 ± 0.042	0.609 ± 0.087	0.644 ± 0.089	0.598 ± 0.017
	D	0.538 ± 0.108	0.420 ± 0.022	0.306 ± 0.022	0.196 ± 0.015
Pancreas	L	7.259 ± 0.766	9.444 ± 2.274	7.499 ± 0.480	7.316 ± 0.946
	D	5.164 ± 1.746	4.246 ± 0.670	2.056 ± 0.173	2.202 ± 0.519
Brain	L	ND	ND	ND	0.800 ± 0.222
	D	ND	ND	ND	0.198 ± 0.022
Tumor	L	1.817 ± 0.127	2.524 ± 0.475	2.719 ± 0.104	2.887 ± 0.192
	D	1.473 ± 0.270	1.731 ± 0.168	1.943 ± 0.197	2.078 ± 0.178

ND = not determined.

Mice ($n = 5$ at each time point) were injected intravenously with 5 MBq of L- or D-^{11}C-CMT via tail vein and killed at 5, 15, 30, and 60 min after injection; tissue samples were rapidly removed, and weight and radioactivity were measured. Data are expressed as SUV.

Both L- and D-^{11}C-MET were <1.0 at 60 min after injection (Fig. 3D). In contrast, the tumor-to-blood ratios of the L-isomers of ^{11}C-CMT and ^{18}F-FMT were 4.4 and 4.0, respectively, and these ratios were markedly improved (5.7 and 7.9, respectively) in the corresponding D-isomers (Figs. 3E and 3F).

Figure 4 shows the incorporation of L- and D-^{11}C-MET, ^{11}C-CMT, and ^{18}F-FMT into the APFs at 60 min after administration in HeLa-bearing mice. As previously expected, L-^{11}C-MET was dominantly detected in the APF in the plasma, liver, pancreas, and tumor, and the incorporation ratios were decreased remarkably by pretreatment with cycloheximide, a protein synthesis inhibitor (Fig. 4A). Although D-^{11}C-MET was found primarily in the ASF in the plasma, tumor, and pancreas, the APF ratios also were decreased significantly by cycloheximide (Fig. 4A). In the L- and D-^{11}C-CMT and ^{18}F-FMT, >95% of the radioactivity was detected in the ASF, but the APF ratios of L-^{11}C-CMT and ^{18}F-FMT revealed a tendency to be decreased by cyclo-

heximide (Figs. 4B and 4C). No significant changes in the APF ratios of D-^{11}C-CMT and ^{18}F-FMT were evident with cycloheximide (Figs. 4B and 4C).

Whole-body imaging with a PPIS provided the consistent distribution data obtained from the tissue dissection assays. Data were displayed as the images accumulated every 10 min, up to 60 min after injection, as shown in Figure 5. Both L- and D-^{11}C-MET accumulated in the abdominal organs, including the liver, pancreas, and spleen (Fig. 5A). In contrast, the D-isomers of ^{11}C-CMT and ^{18}F-FMT showed lower levels in the abdominal regions than those of the corresponding L-isomers (Figs. 5B and 5C). Beside the natural amino acid L-^{11}C-MET, the other unnatural amino acids analogs—especially the D-isomers of ^{11}C-CMT and ^{18}F-FMT—provided a fast and high excretion rate into the bladder via the urine (Fig. 5). As for the uptake into tumor inoculated subcutaneously in the right femoral region, D-^{11}C-MET, L-^{11}C-CMT, and L- and D-^{18}F-FMT accumulated to almost the same level, and L-^{11}C-MET and D-^{11}C-CMT showed

TABLE 3
Uptake of L- and D-^{18}F-FMT in Tumor-Bearing Mice

Organ	Isomer	5 min	15 min	30 min	60 min
Blood	L	1.175 ± 0.024	1.010 ± 0.030	0.852 ± 0.024	0.747 ± 0.029
	D	1.492 ± 0.045	0.699 ± 0.055	0.474 ± 0.018	0.391 ± 0.045
Heart	L	1.180 ± 0.079	1.012 ± 0.025	0.925 ± 0.031	0.838 ± 0.030
	D	1.034 ± 0.024	0.805 ± 0.055	0.608 ± 0.041	0.368 ± 0.014
Lung	L	1.117 ± 0.045	0.923 ± 0.019	0.864 ± 0.007	0.787 ± 0.031
	D	1.332 ± 0.035	0.832 ± 0.038	0.528 ± 0.028	0.325 ± 0.018
Liver	L	1.047 ± 0.014	0.846 ± 0.016	0.815 ± 0.032	0.675 ± 0.025
	D	1.493 ± 0.046	0.738 ± 0.044	0.468 ± 0.013	0.325 ± 0.031
Kidney	L	1.323 ± 0.032	1.177 ± 0.027	1.034 ± 0.052	0.858 ± 0.055
	D	4.550 ± 0.879	1.448 ± 0.083	0.958 ± 0.076	0.610 ± 0.081
Spleen	L	1.533 ± 0.080	1.451 ± 0.088	1.418 ± 0.145	1.070 ± 0.013
	D	1.370 ± 0.046	1.037 ± 0.094	0.805 ± 0.029	0.616 ± 0.259
Muscle	L	1.066 ± 0.069	1.007 ± 0.046	0.842 ± 0.038	0.716 ± 0.015
	D	0.481 ± 0.015	0.575 ± 0.038	0.538 ± 0.014	0.482 ± 0.040
Bone	L	0.929 ± 0.033	0.888 ± 0.026	0.965 ± 0.007	1.143 ± 0.031
	D	0.772 ± 0.016	0.701 ± 0.049	0.713 ± 0.009	0.686 ± 0.042
Intestine	L	1.120 ± 0.033	1.002 ± 0.084	0.837 ± 0.058	0.805 ± 0.074
	D	1.041 ± 0.048	0.718 ± 0.076	0.475 ± 0.062	0.306 ± 0.015
Gut	L	0.898 ± 0.041	1.161 ± 0.666	0.703 ± 0.034	0.609 ± 0.032
	D	0.532 ± 0.040	0.514 ± 0.027	0.353 ± 0.026	0.217 ± 0.020
Pancreas	L	6.601 ± 0.257	7.873 ± 1.088	9.199 ± 0.530	6.243 ± 0.715
	D	7.658 ± 1.621	5.187 ± 1.815	3.853 ± 0.655	2.385 ± 0.264
Brain	L	ND	ND	ND	0.725 ± 0.233
	D	ND	ND	ND	0.382 ± 0.071
Tumor	L	1.478 ± 0.119	2.271 ± 0.457	2.801 ± 0.164	2.700 ± 0.329
	D	1.315 ± 0.248	2.129 ± 0.311	2.489 ± 0.188	2.570 ± 0.547

ND = not determined.

Mice (n = 5 at each time point) were injected intravenously with 5 MBq of L- or D-^{18}F-FMT via tail vein and killed at 5, 15, 30, and 60 min after injection; tissue samples were rapidly removed, and weight and radioactivity were measured. Data are expressed as SUV.

a significantly lower level (Fig. 5). These uptake patterns of these 6 ligands were consistent with the data described in Tables 1–3.

Figure 6 and Table 4 demonstrate the effects of turpentine-induced inflammation on the uptake of ^{18}F-FDG and the D-isomers of ^{11}C-MET, ^{11}C-CMT, and ^{18}F-FMT in tumor-bearing mice, showing that ^{18}F-FDG had a higher accumulation in the inflammatory tissue than that in tumor tissue, whereas no specific uptake of D-^{11}C-MET, D-^{11}C-CMT, and D-^{18}F-FMT was found in the inflammatory tissues.

DISCUSSION

Our study investigated the capability of positron-labeled artificial amino acids, which were not used in protein synthesis, for imaging tumor in vivo using mice bearing HeLa cells. In addition to the comparison between D-^{11}C-MET and its L-isomers, a natural amino acid, the D-isomers of

^{11}C-CMT and ^{18}F-FMT—for which the L-isomers were known to be unnatural amino acids—were compared for evaluation as tumor-imaging agents.

The enantiomeric purity of the positron-labeled amino acids was a critical point for the aim of this study. Evaluation with an optical stereospecific analytic column could certainly confirm that all labeled amino acids used in the present study had an enantiomeric purity of >98%. Ishiwata et al. (22,30) showed earlier that the enantiomeric purity, as well as the radiochemical yield, was affected by the radiolabeling reaction conditions, such as temperature, alkaline concentration, and water content. This result strongly suggested that, even if the L-isomer of ^{11}C-MET, ^{11}C-CMT, or ^{18}F-FMT is subjected to labeling from the corresponding L-type precursor, contamination of the corresponding by-product D-isomers produced during the synthetic procedure should be carefully checked before the injection. Because the behavior of D-^{11}C-MET, ^{11}C-CMT, or ^{18}F-FMT in the normal organs as well as tumor tissues is completely different from

TABLE 4
Uptake of ^{18}F-FDG and D-isomers of ^{11}C-MET, ^{11}C-CMT, and ^{18}F-FMT in Turpentine-Induced Inflammatory Tissue of Tumor-Bearing mice

Organ	^{18}F-FDG	D-^{11}C-MET	D-^{11}C-CMT	D-^{18}F-FMT
Blood	0.239 ± 0.049	0.523 ± 0.064	0.405 ± 0.032	0.391 ± 0.045
Tumor	0.997 ± 0.064	3.087 ± 0.487	2.078 ± 0.178	2.570 ± 0.547
T/B	4.291 ± 0.064	5.902 ± 0.304	5.131 ± 0.344	6.573 ± 0.486
Muscle	0.437 ± 0.062	0.607 ± 0.037	0.462 ± 0.033	0.482 ± 0.040
M/B	1.759 ± 0.224	1.125 ± 0.023	1.396 ± 0.045	1.294 ± 0.096
Inflammation	1.157 ± 0.123	0.657 ± 0.057	0.429 ± 0.005	0.470 ± 0.085
I/B	4.895 ± 0.485	1.202 ± 0.046	1.117 ± 0.022	1.356 ± 0.125

T/B = tumor-to-blood ratio; M/B = muscle-to-blood ratio; I/B = inflammatory tissue-to-blood ratio.

Mice (n = 5 at each time point) were injected intravenously with 5 MBq of labeled ligand via tail vein and killed at 60 min after injection; tissue samples were rapidly removed, and weight and radioactivity were measured. Data in blood, tumor, muscle, and inflammatory tissue are expressed as SUV.

that of the corresponding L-isomer—as demonstrated in the previous study (20) and the present study—the mixture of these 2 isomers might mislead the diagnosis of tumor grading and therapeutic efficacy when determined on the basis of the uptake values of the tracers.

In general, the tumor uptake is thought to reflect the increased uptake of amino acid in tumor cells, including the facilitated active transport, metabolism, and activated protein synthesis rate. However, is well known that natural L-amino acids are also used avidly by normal organs, which does hamper the tracers' utility as tumor-imaging agents because of the lower tumor-to-normal organ ratio. Furthermore, L-^{11}C-MET is known to be incorporated not only into proteins via the conversion into amino-acyl-tRNA but also into nonprotein materials, such as lipids and RNA by the transmethylation process via S-adenosyl-L-methionine (3). This study confirmed the use of L-^{11}C-MET for protein synthesis by showing the remarkable reduction of L-^{11}C-MET uptake into the APF by pretreatment with cycloheximide, a protein synthesis inhibitor. In contrast, the previous reports have emphasized that an advantage of labeled unnatural amino acids, such as L-^{11}C-CMT and L-^{18}F-FMT, was the relatively lower uptake in the abdominal organs than that of L-^{11}C-MET (17), and the present study revealed that only small amounts of L-^{11}C-CMT and L-^{18}F-FMT were detected

in the protein fraction. Although pretreatment with cycloheximide decreased slightly the incorporation of L-^{11}C-CMT and L-^{18}F-FMT into the protein fraction, it did not hamper their capacity as tumor-imaging agents because the baseline-use levels were almost negligible as the precursors of protein synthesis. Taken together from the comparison data of the L- and D-isomers of ^{11}C-MET, ^{11}C-CMT, and ^{18}F-FMT—including the facilitated active amino acid transport, metabolism, and activated protein synthesis rate in tumor tissue—the transport process into the amino acid pool, not the protein synthesis phase, was considered to be a critical target for better tumor imaging.

On the basis of this concept, we tried to evaluate the D-isomeric amino acid analogs that were reported to be taken up primarily into the acid-soluble amino acid pool, not into the acid-precipitable protein fraction (23,24,31–34). Among D-^{11}C-MET, ^{11}C-CMT, and ^{18}F-FMT assayed here, D-MET had already been reported to be a potential tumor-imaging agent using ^{14}C-labeled MET (23). With regard to properties in the blood, D-^{11}C-MET showed a higher blood level, faster clearance rate, greater stability against metabolism, and lower protein incorporation ratio than L-^{11}C-MET, a natural amino acid, all of which were consistent with the earlier report (23). Of interest, the present result showed that a fairly large portion of radioactivity from D-^{11}C-MET was
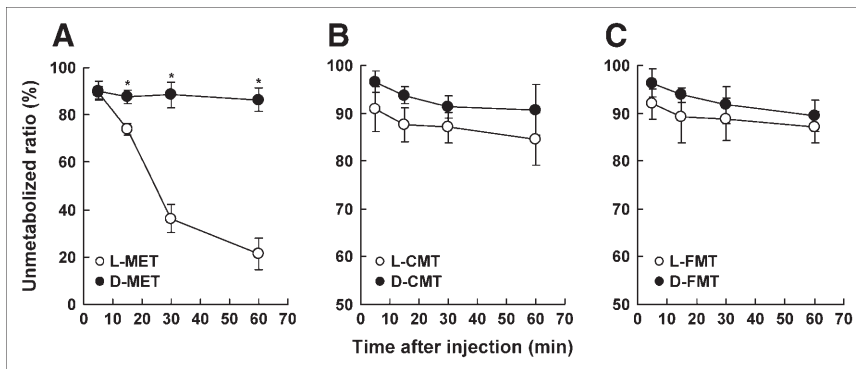
FIGURE 2. Metabolic analyses of L- and D-isomers of ^{11}C-MET (A), ^{11}C-CMT (B), and ^{18}F-FMT (C) in plasma. At each time point after injection, plasma samples were prepared, and samples obtained were developed on TLC plates using a mobile phase of *n*-buthanol/acetic acid/PBS (pH 7.4; 4:1:2). The ratio of radioactivity in the unmetabolized fraction to that in total plasma (metabolized plus unmetabolized) was determined using a phosphoimaging plate. *$P < 0.05$ vs. corresponding L-isomer.
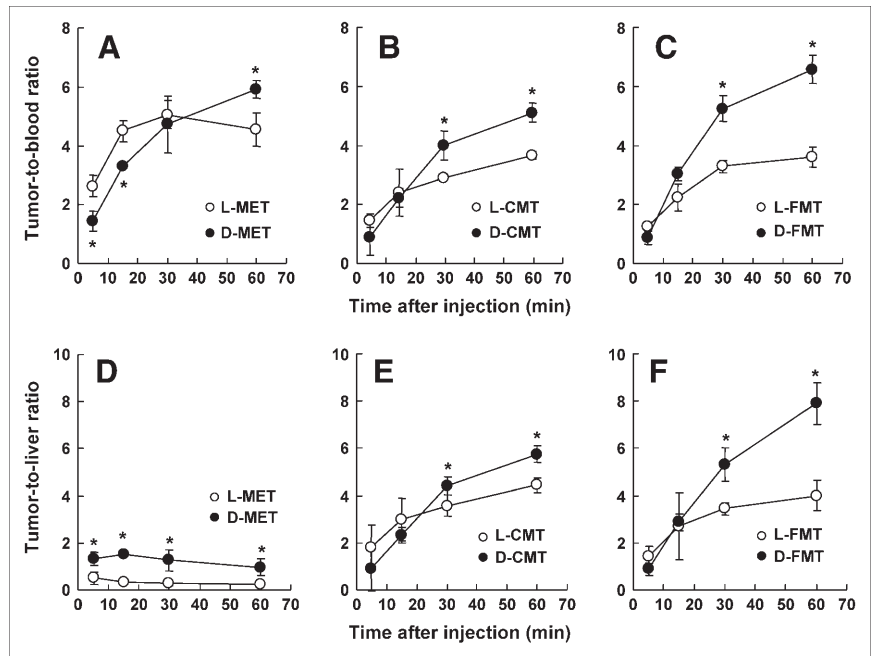
FIGURE 3. Time course of tumor-to-blood ratios (A–C) and tumor-to-liver ratios (D–F) of L- and D-isomers of ^{11}C-MET (A and D), ^{11}C-CMT (B and E), and ^{18}F-FMT (C and F) in HeLa-bearing mice. Ratios of the SUV of tumor against the SUV of blood or liver were determined and plotted against time after injection. *$P < 0.05$ vs. corresponding L-isomer.

found in the acid-precipitable protein fraction, which was further decreased by the preadministration of cycloheximide, suggesting that the use of D-^{11}C-MET in protein synthesis may not be negligible. It has been reported that many animal species have D-amino acid oxidase, by which D-^{11}C-MET might be partially converted to α-keto-γ-methiolbutyrate, followed by transamination to its L-isomer (31,32). The high blood level, attributed to greater stability in the plasma, as well as the lower, but still not negligible, use for protein synthesis of D-^{11}C-MET, might be attributable to less improvement of the tumor-to-blood and tumor-to-liver ratios in comparison with L-^{11}C-MET. In contrast to D-^{11}C-MET, the D-isomers of ^{11}C-CMT and ^{18}F-FMT had lower blood levels and much faster clearance rates than the corresponding L-isomers and comparable stability against metabolism and almost equivalent very low incorporation ratios into the protein fraction with the corresponding L-isomers. These properties of the D-isomers of ^{11}C-CMT and ^{18}F-FMT provided the much better tumor-to-blood and tumor-to-liver ratios than the corresponding L-isomers.

As described earlier, most natural amino acids are distributed into the free amino acid pool of tumor tissue across the plasma membranes and some are used in protein synthesis. Several results have suggested that amino acid transport, rather than protein synthesis, is the dominant accumulation process (15,17,35). In peripheral tissues and tumors, leucine and tyrosine are taken up by the L-transport (leucine preferring) system and MET is taken up by both the L and the A (alanine preferring) system (36,37). Our study with cycloheximide demonstrated the reduced incorporation of L- and D-^{11}C-MET into the protein fraction but no significant changes in the incorporation of the D-isomers of ^{11}C-CMT and ^{18}F-FMT. These results strongly suggest that the D-isomers of ^{11}C-CMT and ^{18}F-FMT are useful tracers for tumor imaging because the
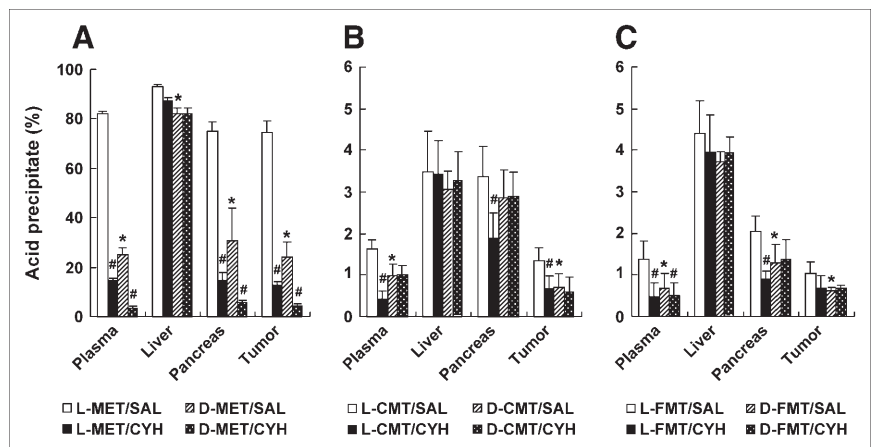
FIGURE 4. Assessment of protein incorporation ratios (PIP (%)) of L- and D-isomers of ^{11}C-MET (A), ^{11}C-CMT (B), and ^{18}F-FMT (C) in HeLa-bearing mice. Cycloheximide (CYH; 100 mg/kg body weight) was administered intraperitoneally 30 min before tracer injection; animals were killed 60 min after injection. Incorporation of radioactivity into proteins was determined as 7.5% TCA-precipitable fractions in plasma, liver, pancreas, and tumor, and PIP values were calculated. *$P < 0.05$ vs. corresponding L-isomer; #$P < 0.05$ vs. corresponding saline (SAL) condition.
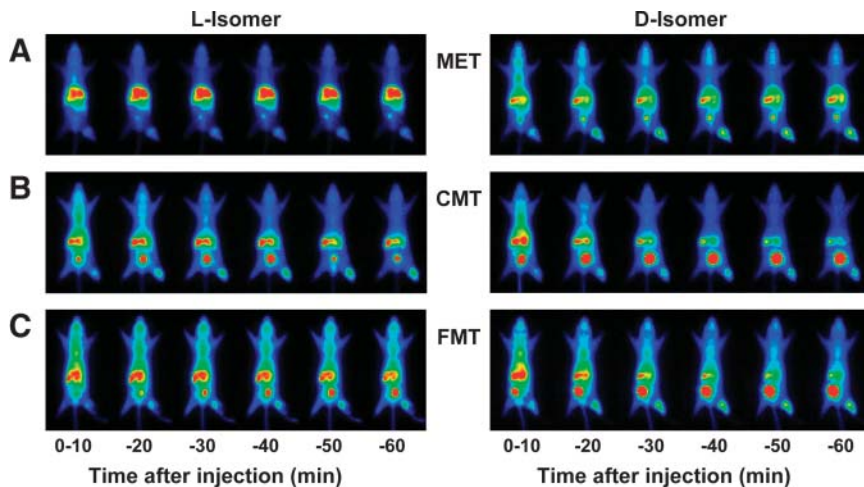
FIGURE 5. Whole-body imaging of L- and D-isomers of ^{11}C-MET (A), ^{11}C-CMT (B), and ^{18}F-FMT (C) in tumor-bearing mice with PPIS. Two mice anesthetized with chloral hydrate were positioned prone on an acrylic plate and placed on the midplane between 2 opposing detectors arranged in a horizontal mode. Each radiolabeled compound at a dose of 1 MBq was injected intravenously into each mouse via the tail vein. Data were acquired with a 1-min time frame interval for 60 min after injection, and 6 summation images were created every 10 min.

uptake of these tracers could predominantly reflect the membrane transport capacity from the plasma to the amino acid pool rather than incorporation into proteins.

Whole-body imaging of tumor-bearing mice with a PPIS (27) further indicated that the application of the D-isomers could alter the distribution and kinetic properties of ^{11}C-MET, ^{11}C-CMT, and ^{18}F-FMT in the abdominal normal organs and tumor tissues. In general, the distribution and kinetic patterns were in good agreement with the data obtained with the tissue dissection method. The images visually revealed that the L-isomers of ^{11}C-CMT and ^{18}F-FMT were rapidly cleared from the liver and excreted into the bladder as urine via the kidneys, which was the property found in other artificial amino acids (17,18,20,22). We noted that whole-body imaging is very useful in evaluating whether a novel tracer is promising for tumor detection. For example, as shown in Table 3, the absolute SUVs of L- and D-^{18}F-FMT in the tumor were comparable; however, whole-body imaging with D-^{18}F-FMT showed tumor tissue much

better than that with L-^{18}F-FMT. This indicated that the relatively high uptake in the tumor tissue and the low level in normal organs result in a higher capability for tumor detection with improved normal tumor-to-tissue ratios.
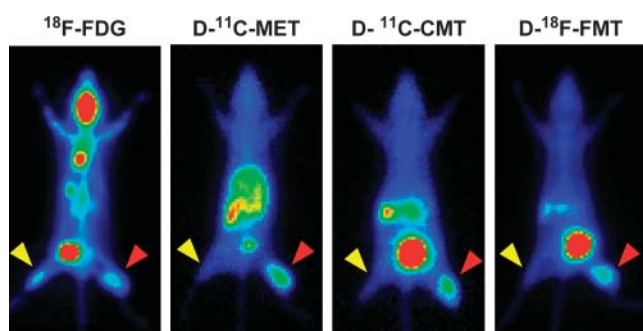
CONCLUSION

This study demonstrated that the D-isomers of ^{11}C-CMT and ^{18}F-FMT were better than the corresponding L-isomers as tumor-detecting agents with PET in comparison with L- and D-^{11}C-MET. Because the rapid excretion from the ASF into the urine—due to less protein use—results in a higher tumor-to-blood ratio as well as less radiation hazards in subjects, the labeled tyrosine analogs D-^{11}C-CMT and D-^{18}F-FMT are expected to be better imaging agents for cerebral and peripheral tumors than labeled natural amino acids.

FIGURE 6. Effects of inflammation on uptake of ^{18}F-FDG and D-isomers of ^{11}C-MET, ^{11}C-CMT, and ^{18}F-FMT in HeLa-bearing mice. HeLa cells were inoculated in right hind legs 2 wk before tracer injection (red arrowheads), and turpentine (0.05 mL) was administered subcutaneously in left hind legs 3 d before tracer injection (yellow arrowheads). Mice were imaged with PPIS for 60 min after injection of ^{18}F-FDG, D-^{11}C-MET, D-^{11}C-CMT, and D-^{18}F-FMT, and the accumulated images from 41 to 60 min after injection were created.

REFERENCES

1. Kubota R, Kubota K, Yamada S, Tada M, Ido T, Tamahashi N. Microautoradiographic study for differentiation of intratumoral macrophages, granulation tissue and cancer cells by the dynamic fluoro-18-fluorodeoxyglucose uptake. *J Nucl Med.* 1994;35:104–112.
2. Bolster JW, Vaalburg W, Elsinga PH, Wijnberg H, Woldring MG. Synthesis of DL-[1-^{11}C]methionine. *Appl Radiat Isot.* 1986;37:1069–1070.
3. Ishiwata K, Vaalburg W, Elsinga PH, Paans AMJ, Woldring MG. Comparison of L-[1-^{11}C]methionine and L-methyl-[^{11}C]methionine for measuring in vivo protein synthesis rates with PET. *J Nucl Med.* 1988;29:1419–1427.
4. Comar D, Cartron JC, Maziere M, Marazano C. Labeling and metabolism of methionine-methyl-[11]C. *Eur J Nucl Med.* 1976;1:11–14.
5. Långström B, Antoni G, Gulberg P, et al. Synthesis of L- and D-[methyl-^{11}C]methionine. *J Nucl Med.* 1987;28:1037–1040.

6. Halldin C, Schoeps KO, Stone-Elander S, Wiesel FA. The Bucherer–Strecker synthesis of D- and L-[1-^{11}C]tyrosine and the in vivo study of L-[1-^{11}C]tyrosine in human brain using positron emission tomography. *Eur J Nucl Med.* 1987;13: 288–291.

7. Ishiwata K, Vaalburg W, Elsinga PH, Paans AMJ, Woldring MG. Metabolic studies with L-[^{11}C]tyrosine for the investigation of a kinetic model to measure protein synthesis rates with PET. *J Nucl Med.* 1988;29:524–529.

8. Bjurling P, Watanabe Y, Oka S, Nagasawa T, Yamada H, Långström B. Multienzymatic synthesis of β-^{11}C-labelled L-tyrosine and L-DOPA. *Acta Chem Scand.* 1990;44:183–188.

9. Hawkins RA, Huang SC, Barrio JR, et al. Estimation of local cerebral protein synthesis rates with L-[1-^{11}C]leucine and PE: methods, model and results in animals and humans. *J Cereb Blood Flow Metab.* 1989;9:446–460.

10. Casey DL, Digenis GA, Wesner DA, et al. Preparation and preliminary tissue studies of optically active D- and L-[^{11}C]phenylalanine. *Int J Appl Radiat Isot.* 1981;32:1291–1300.

11. Barrio JR, Keen RE, Chugani H, Ackerman R, Chugani D, Phelps ME. L-[^{11}C]Phenylalanine for the determination of cerebral protein synthesis rates in man with positron emission tomography [abstract]. *J Nucl Med.* 1983; 24(suppl):P70.

12. Lemaire C, Guillaume M, Christiaens L, Palmer AJ, Cantineau R. A new route for the synthesis of [^{18}F]fluoroaromatic substituted amino acids: no carrier acids L-p-[^{18}F]fluorophenylalanine. *Int J Rad Appl Instrum [A].* 1987;38:1033–1038.

13. Coenen HH, Kling P, Stöcklin G. Cerebral metabolism of L-[2-^{18}F]fluorotyrosine, a new PET tracer of protein synthesis. *J Nucl Med.* 1989;30:1367–1372.

14. Wienhard K, Herholz K, Coenen HH, et al. Increased amino acid transport into brain tumors measured by PET of L-(2-^{18}F)fluorotyrosine. *J Nucl Med.* 1991;32: 1338–1346.

15. Vaalburg W, Coenen HH, Crouzel, et al. Amino acids for the measurement of protein synthesis in vivo by PET. *Nucl Med Biol.* 1992;19:227–237.

16. Iwata R, Furumoto S, Pascali C, Bogni A, Ishiwata K. Radiosynthesis of O-[^{11}C]methyl-L-tyrosine and O-[^{18}F]fluoromethyl-L-tyrosine as potential PET tracer for imaging amino acid transport. *J Labelled Compds Radiopharm.* 2003;46: 555–566.

17. Ishiwata K, Kawamura K, Wang WF, et al. Evaluation of O-[^{11}C]methyl-L-tyrosine and O-[^{18}F]fluoromethyl-L-tyrosine as tumor imaging tracers by PET. *Nucl Med Biol.* 2004;31:191–198.

18. Wester HJ, Herz M, Weber W, et al. Synthesis and radiopharmacology of O-(2-[^{18}F]fluoroethyl)-L- tyrosine for tumor imaging. *J Nucl Med.* 1999;40:205–212.

19. Heiss P, Mayer S, Herz M, Wester HJ, Schwaiger M, Senekowitsch-Schmidtke R. Investigation of transport mechanism and uptake kinetics of O-(2-[^{18}F]fluoroethyl)-L-tyrosine in vitro and in vivo. *J Nucl Med.* 1999;40:1367–1373.

20. Tang G, Tang X, Wang M, Luo L, Gan M. Fully automated synthesis of O-(3-[^{18}F]fluoropropyl)-L-tyrosine by direct nucleophilic exchange on a quaternary 4-aminopyridium resin. *Appl Radiat Isot.* 2003;58:685–689.

21. Tang G, Wang M, Tang X, Luo L, Gan M. Synthesis and evaluation of O-(3-[^{18}F]fluoropropyl)-L-tyrosine as an oncologic PET tracer. *Nucl Med Biol.* 2003; 30:733–739.

22. Ishiwata K, Kasahara C, Hatano K, Ishii S, Senda M. Carbon-11 labeled ethionine and propionine as tumor detecting agents. *Ann Nucl Med.* 1997;11: 115–122.

23. Takeda A, Goto R, Tamemasa O, Chaney JE, Digenis GA. Biological evaluation of radiolabeled D-methionine as a parent compound in potential nuclear imaging. *Radioisotopes.* 1984;33:213–217.

24. Tamemasa O, Goto R, Takeda A, Maruo K. High uptake of ^{14}C-labeled D-amino acids by various tumors. *Gann.* 1982;73:147–152.

25. Schober O, Duden C, Meyer GJ, Muller JA, Hundeshagen H. Non selective transport of [^{11}C-methyl]-L- and D-methionine into a malignant glioma. *Eur J Nucl Med.* 1987;13:103–105.

26. Bergström M, Lundqvist H, Ericson K, et al. Comparison of the accumulation kinetics of L-(methyl-^{11}C)-methionine and D-(methyl-^{11}C)-methionine in brain tumor studies with positron emission tomography. *Acta Radiol.* 1987;28:225–229.

27. Uchida H, Okamoto T, Ohmura T, et al. A compact planar positron imaging system. *Nucl Instrum Methods Phys Res A.* 2004;A516:564–574.

28. Oberdorfer F, Hull WE, Traving BC, Maier-Borst W. Synthesis and purification of 2-deoxy-2-[18]fluoro-D-glucose and 2-deoxy-2-[18]fluoro-D-mannose: characterization of products by ^{1}H and ^{19}F-NMR spectroscopy. *Int J Appl Radiat Isot.* 1986;37:695–700.

29. Yamada S, Kubota K, Kubota R, Ido T, Tamahashi N. High accumulation of fluorine-18-fluorodeoxyglucose in turpentine-induced inflammatory tissue. *J Nucl Med.* 1995;36:1301–1306.

30. Ishiwata K, Ido T, Vaalburg W. Increased amount of D-enantiomer dependent on alkaline concentration in the synthesis of L-[methyl-^{11}C]methionine. *Appl Radiat Isot.* 1988;39:311–314.

31. Berg CP. Physiology of the D-amino acids. *Physiol Rev.* 1953;33:145–189.

32. Steginck LD, Moss J, Printen KJ, Cho ES. D-Methionine utilization in adult monkeys fed diets containing DL-methionine. *J Nutr.* 1980;110:1240–1246.

33. Goto R, Tezuka M, Tamemasa O. Incorporation of L-, D-, and DL-amino acids in to the pancreas of mice. *Chem Pharm Bull* (Tokyo). 1977;25:1574–1581.

34. Tamemasa O, Digenis GA, Tezuka M, Takeda A, Chaney LE, Goto R. Differential radioactivity uptake from ^{14}C-labeled D- and L-leucine by the pancreas of animals pretreated with pancreatitis-causing agents. *Chem Pharm Bull* (Tokyo). 1982;30:2521–2528.

35. Kubota K, Yamada K, Fukuda H, et al. Tumor detection with carbon-11-labelled amino acids. *Eur J Nucl Med.* 1984;9:136–140.

36. Oxender DL, Christensen HN. Distinct mediating system for the transport of natural amino acids by the Ehrlich cell. *J Biol Chem.* 1963;238:3686–3699.

37. Christensen HN. On the development of amino acid transport system. *Fed Proc.* 1973;32:19–28.